Electronic Supplementary Material (ESI) for Journal of Materials Chemistry B.

Supporting Information

Dual Ligand-Assisted Assembly of Metal-Organic Frameworks on Upconversion Nanoparticles for NIR Photodynamic Therapy against Hypoxic Tumors

Xinyue Zhang[†a], Jiasen Cui[†b], Jinhui Liu[a], Xi Chen[b], Mingli Chen*[a], Jianhua Wang*[a]

a Department of Chemistry, College of Sciences, Northeastern University, Box 332, Shenyang, 110819, China.

b School and Hospital of Stomatology, Department of Oral Pathology, China Medical University, Liaoning Provincial Key Laboratory of Oral Diseases, Shenyang, 110001, China.

***Corresponding author**

Jianhua Wang. E-mail: jianhuajrz@mail.neu.edu.cn (J.-H. Wang)

Mingli Chen. E-mail: chenml@mail.neu.edu.cn (M.-L. Chen)

Tel.: +86 24 83688944. Fax: +86-24-83688944.

† These authors contributed equally to this study.

Table of Contents

Experimental

Chemicals and Reagents

Dimethylformamide (DMF), polyvinyl pyrrolidone (PVP, Mw = 40 000), branched polyethylenimine (PEI, Mw = 10 000), benzoic acid (BA), Zirconium(IV) chloride ($ZrCl_2$ 99.99%), ytterbium chloride hexahydrate ($YbCl_3 \cdot 6H_2O$, 99.99%), yttrium chloride hexahydrate ($YCl_3 \cdot 6H_2O$, 99.99%), thulium chloride hexahydrate ($TmCl_3 \cdot 6H_2O$, 99.99%), neodymium chloride hexahydrate ($NdCl_3 \cdot 6H_2O$, 99.99%), ammonium fluoride (NH_4F, 99.99%), oleic acid (OA), 1-octadecene (ODE), 9,10-Anthracenediyl-bis(methylene)dimalonic acid (ABDA), 1,3-Diphenylisobenzofuran (DPBF) and 2,7-Dichlorodihydrofluorescein diacetate (DCFH-DA) were obtained from Aladdin. Fe (III) meso-tetra(4-carboxyphenyl) porphine chloride (Fe(III)-TCPP) was provided from Bidepharm. Propidium Iodide (PI) was acquired from Biosharp. Fluorescein Diacetate (FDA) and 4',6-diamidino-2-phenylindole (DAPI) were purchased from Solarbio. Cell Counting Kit-8 (CCK-8) was bought from Seven. $[Ru(dpp)_3]$ Cl_2 was received from Macklin. Singlet Oxygen Sensor Green reagent (SOSG) was obtained from Meilunbio. All chemical reagents of analytical grade were used directly without further purification.

Cell lines and animals' model

HepG2 cells were incubated in DMEM supplemented with 10% FBS and 1%antibiotics (penicillin-streptomycin, 10,000 U/mL) at 37 °C under 5% CO_2. Male BALB/c mice aged 7 weeks were purchased from SPF Biotechnology Co, LTD. (Beijing, China) and were subcutaneously injected with HepG2 cells to establish a xenograft model in nude mice.

This study was approved by the Animal Ethics and Review Committee of China Medical University (approval number: CMU2022164, approval day: July 19, 2022).

Apparatus

The images of TEM and elemental mappings were carried out by a Tecnai G20 (FEI, Netherlands). The images of SEM were obtained on a SU8010 scanning electron microscope (Hitachi High Technologies, Japan). The XRD patterns were obtained by Empyrean X-ray Diffractometer (Panalytical Ltd, Netherlands). Fourier transform infrared (FTIR) spectra were recorded on a Nicolet-6700 spectrophotometer (Thermo Instruments Inc., USA). The zeta-potentials were measured by a Zetasizer Nano ZS/ZEN3690 instrument (Malvern, England). X-ray photoelectron spectroscopy (XPS) scanning curves were obtained on an ESCALAB 250 surface analysis platform (Thermo Electron). Fluorescence spectra were obtained by using an Edinburgh FLS 980 (Edinburgh, UK). Ultraviolet/visible (UV/vis) absorption spectra were recorded using a U-3900 UV/vis spectrophotometer (Hitachi, Japan). Upconversion emission spectra was collected on the Flame UV-VIS Spectrometer (Ocean Insight, America) quipped with a 980nm NIR laser as the excitation source (Changchun New Industries Optoelectronics Technology Co., Ltd., China). ESR spectra of UCMs were measured by Bruker A300 (Bruker, Germany). Fluorescence images were observed by confocal laser scanning microscopy (CLSM) FV1200 (Olympus, Japan). Flow cytometric analysis was performed on a BD Accuri C6 Plus flow cytometer (Becton, Dickinson and Company, America).

The $^1O_2$ generation test

Singlet oxygen was detected by SOSG. At first, sample solutions (200 μg/mL) were mixed with SOSG (5 mM, 2 μL) and the solution was irradiated with a 980 nm laser (1.5 W/cm^2) under different treatments for 10 min (The concentration of H_2O_2 was 100 μM). The fluorescence of each sample was then detected to determine the production of $^1O_2$ by a fluorimeter. In addition, ABDA was employed for measuring $^1O_2$ production at different times under laser irradiation (1.5 W/cm^2). ABDA solution (2.5 mM) was added into of UCMs in PBS solution, and mixture was then irradiated with a 980 nm laser for different periods (0-10 min, measured every 2 min) to measure the production of $^1O_2$ by monitoring the change in absorbance of ABDA.

The $^1O_2$ quantum yields by UCMs

To calculate the quantum yield of singlet oxygen generation from UCMs, 1,3-Diphenylisobenzofuran (DPBF) was used as an indicator of $^1O_2$ generation. The $^1O_2$ quantum yield ($\Delta\varphi$) was calculated by monitoring the oxidation of DPBF with a UV-Vis spectrophotometer. Methylene blue (MB, $\Delta\varphi_{std} = 0.52$) was used as the standard substance to determine the quantum yield [1,2]. Both MB and porphyrin MOFs can absorb the light at 660 nm and generate $^1O_2$. Briefly, the irradiation was performed with 660 nm LED light (83.2 mW/cm^2) in MB (2 μM) and UCMs (2 μM) containing 60 μM DPBF. The absorbance of DPBF was monitored at different time points. The quantum yield of $^1O_2$ is calculated by the following equation: x: UCMs; std: MB; S: the slope of the absorbance of

DPBF (420 nm) and irradiation time; F: absorption correction factor, F = 1 - 10^{-OD} (OD: the optical density of UCMs and MB at 660 nm).

$$\varphi_{\triangle} = \varphi_{\triangle(std)} \times \frac{S_X}{S_{std}} \times \frac{F_{std}}{F_X}$$

Cytotoxicity text

CCK-8 was used to analyze cytotoxicity. HepG2 cells were seeded in 96-well plates and cultured for 24 h. The medium solutions containing different concentrations of UCMs (0, 20, 40, 60, 80, 100, 120, 140, 160, 180, 200, 400, 600, 800, 1000 μg/mL) were added and the cells were cultured continuously for 24 h. Afterwards, 10 μL of CCK-8 solution was added to each well, Followed by further incubation for 1-4 h. Finally, the absorbance at 450 nm was determined with a microplate reader.

Detection of O_2 production *in vitro*

The O_2 generation ability of UCMs *in vitro* can be detected by using $[Ru(dpp)_3]Cl_2$. To simulate the tumor hypoxic environment, HepG2 cells were incubated in oxygen-depleted bags for 12 h, and then 100 μL of $[Ru(dpp)_3]Cl_2$ (50 μM) solution was added into the cells and continued to incubate for another 4 h. Then, cells were treated with different conditions and incubated for 30 min (UCMs: 100 μg/mL; H_2O_2: 100 μM). Finally, the cells were stained with DAPI for 15 min and observed from confocal laser scanning microscope.

ROS generation test *in vitro*

ROS in cells were measured by DCFH-DA. HepG2 cells were seeded and cultured in confocal culture dishes overnight. After 12 h incubation at 37 °C, the cells were treated with different conditions and then incubated for a further 4 h, and the NIR was irradiated

with a 1.5 W/cm^2 980 nm laser for 10 min. Then the medium was removed, followed by the addition of DCFH-DA and DAPI. The culture medium was removed after 20 min incubation, and the strips were washed three times with PBS. Fluorescence images of the cells was analyzed by confocal laser scanning microscope.

In vivo biodistribution of UCMs

To assess the biodistribution, mice were injected at the tailbone with UCMs. Brain, liver, kidney, spleen and lung tissues were collected from the mice at 6 h, 24 h and 48 h after injection. The collected organs and tissues were weighed and dissolved in 3 mL of nitric acid and 1 mL of hydrogen peroxide for 12 h. Deionized water was diluted and measured by ICP-MS.

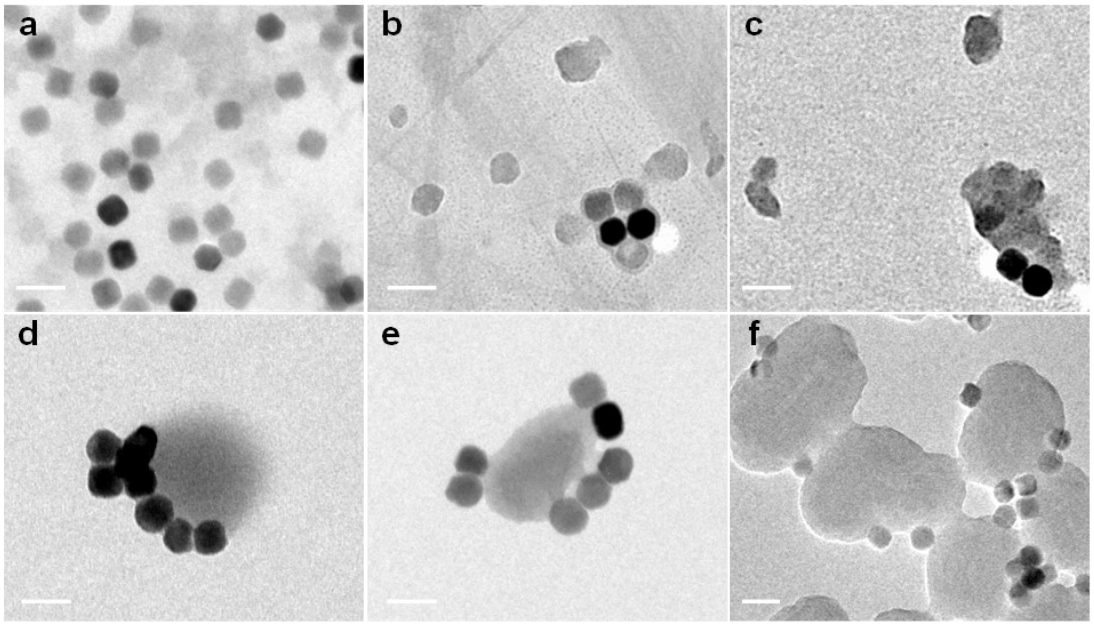

Figure S1. TEM images of the UCMs obtained at various reaction times. (a) 1 min, (b) 5 min, (c) 4 h (begin to heat), (d) 5 h, (e) 9 h, (f) 10 h. The scale bars indicate 50 nm.

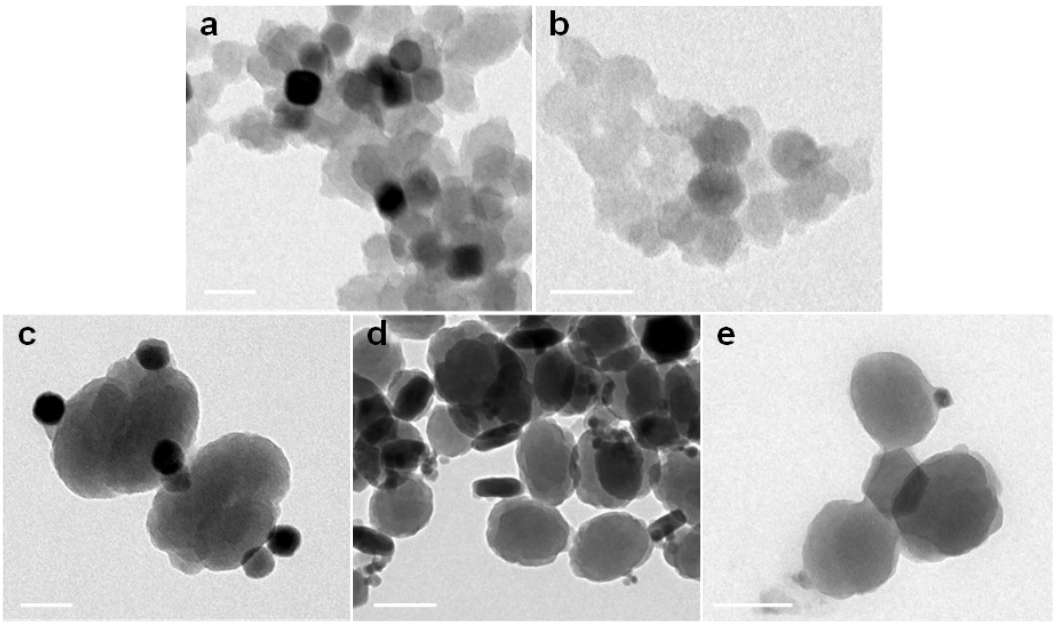

Figure S2. Effect of the mass ratio of ligands on the synthesis of UCMs nanoparticles. (a) The modification with only PEI, (b) The modification with PEI and PVP with a mass ratio of m(PEI/PVP) = 1/1, (c) The modification with PEI and PVP with a mass ratio of m(PEI/PVP) = 1/2, (d) The modification with PEI and PVP with a mass ratio of m(PEI/PVP) = 1/10, (e) The modification with only PVP. The scale bars indicate 50 nm.

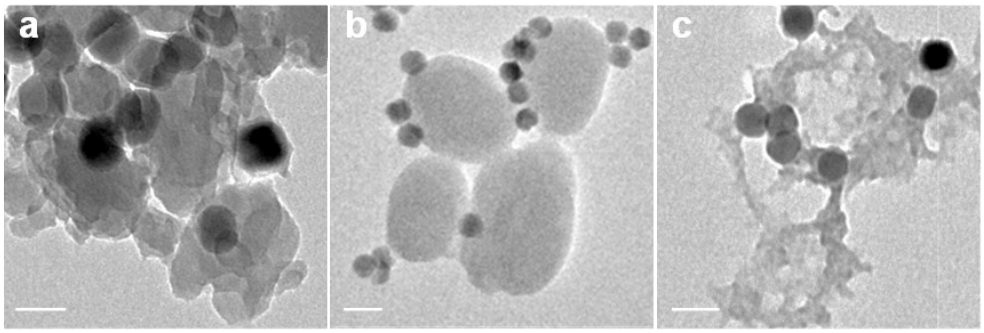

Figure S3. TEM images of the UCNPs/MOFs hybrid structures synthesized in (a) DMF/ethanol (V/V = 1/1) solution, (b) DMF/ethanol/methanol (V/V/V = 2/1/1) solution, (c) ethanol/methanol (V/V = 1/1) solution. The scale bars indicate 50 nm.

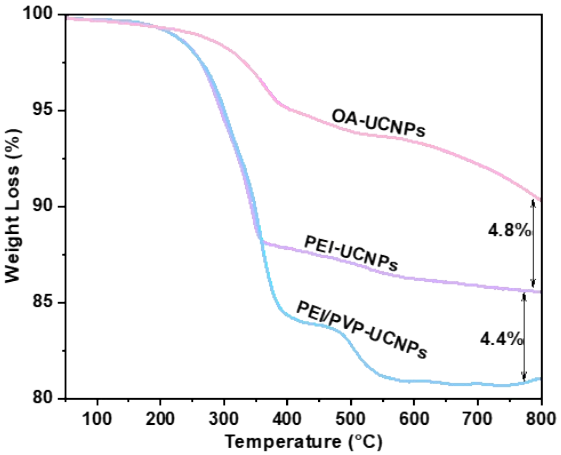

Figure S4. TGA curves obtained for OA-UCNPs, PEI-UCNPs and PEI/PVP-UCNPs.

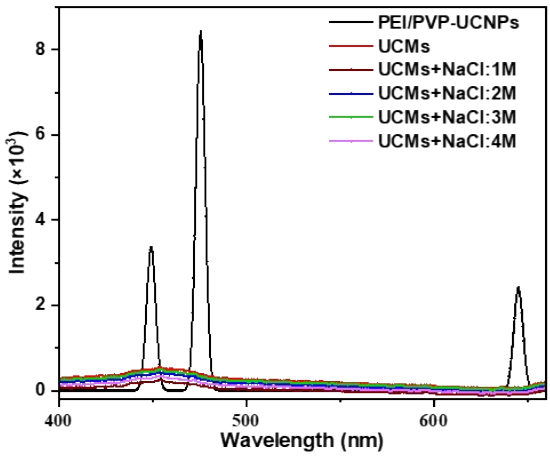

Figure S5. Stability of UCMs (1 mg/mL) in the presence of different concentrations of sodium chloride tested by the upconversion luminescence spectra under 980 nm laser irradiation. (1.5 W/cm^2)

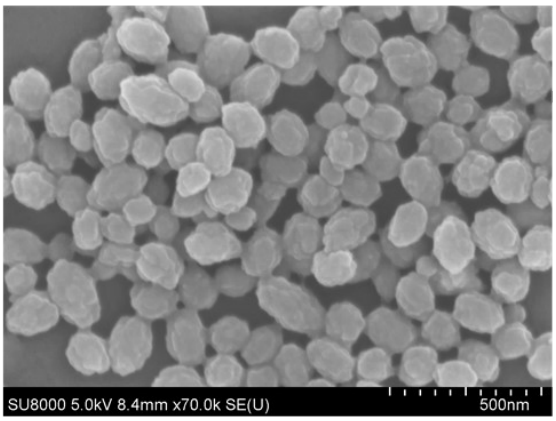

Figure S6. SEM image of PCN-224(Fe) obtained with the same method for the synthesis of UCMs.

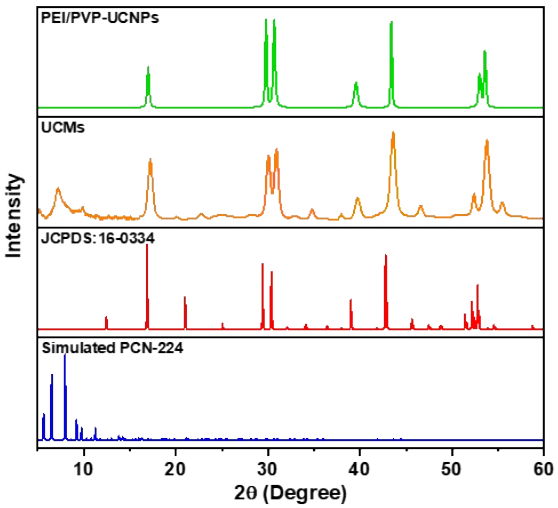

Figure S7. XRD patterns of PEI/PVP-UCNPs and UCMs contrasted with standard JCPDS:16-0334 and simulated PCN-224 separately.

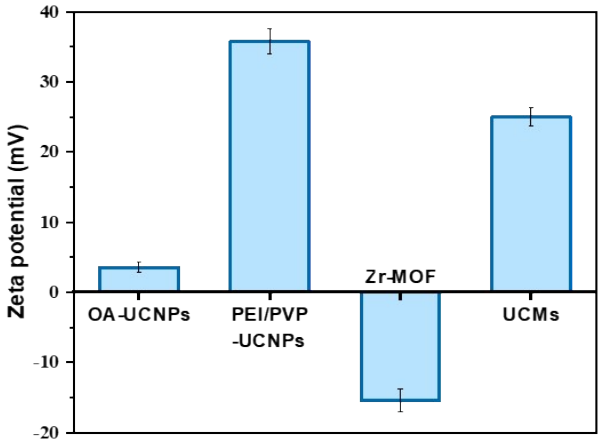

Figure S8. The variation of zeta potentials for the reaction systems during the preparation process of UCMs.

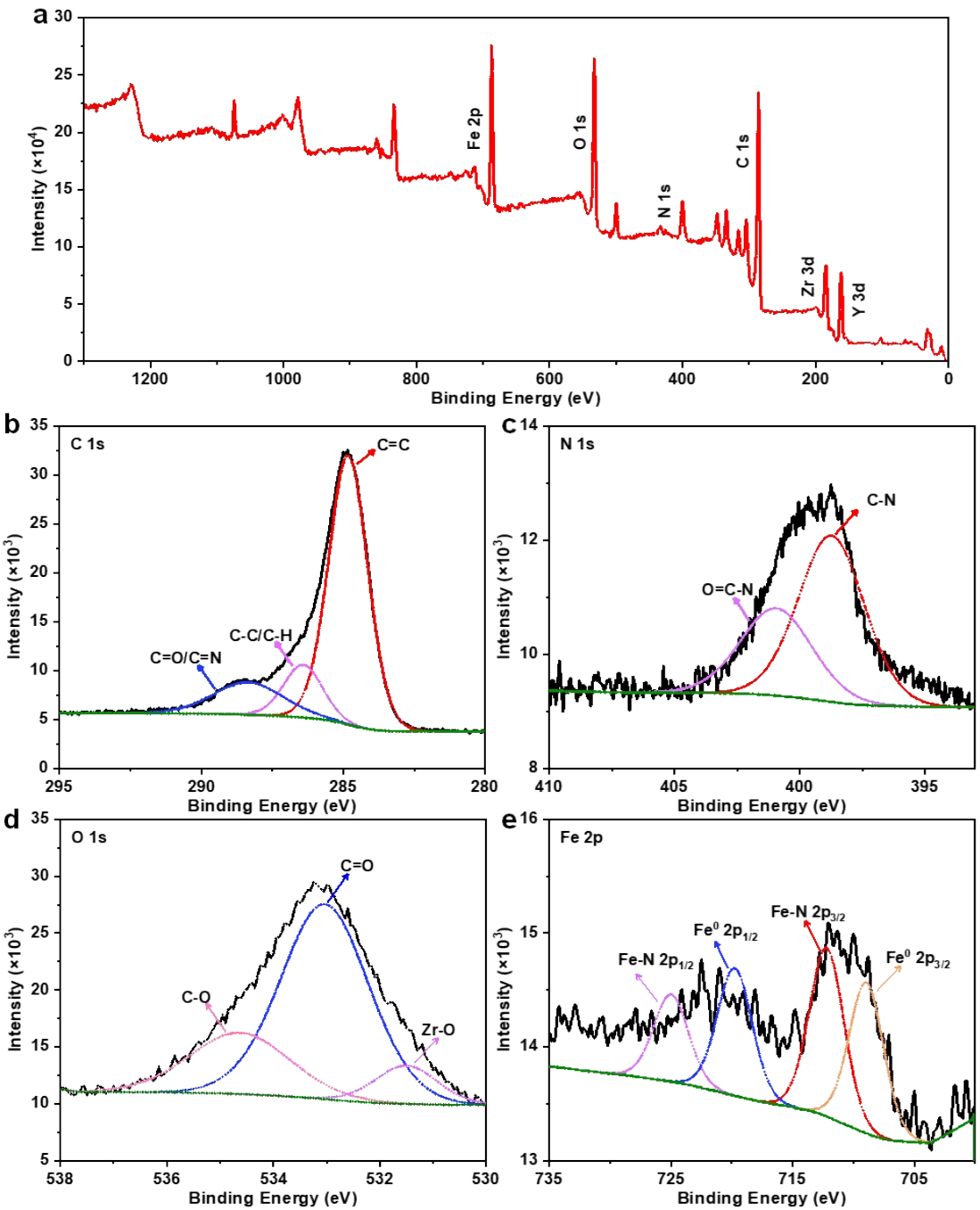

Figure S9. (a) XPS spectrum of UCMs. High-resolution XPS spectra of (b) C 1s, (c) N 1s, (d) O 1s and (e) Fe 2p.

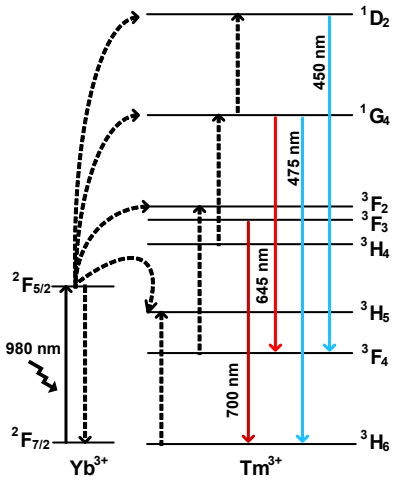

Figure S10. Schematic illustration of the energy-transfer mechanism for $NaYF_4$:25% Yb^{3+}, 0.9% Tm^{3+}, 0.6% Nd^{3+} UCNPs with excitation multicolor upconversion luminescence.

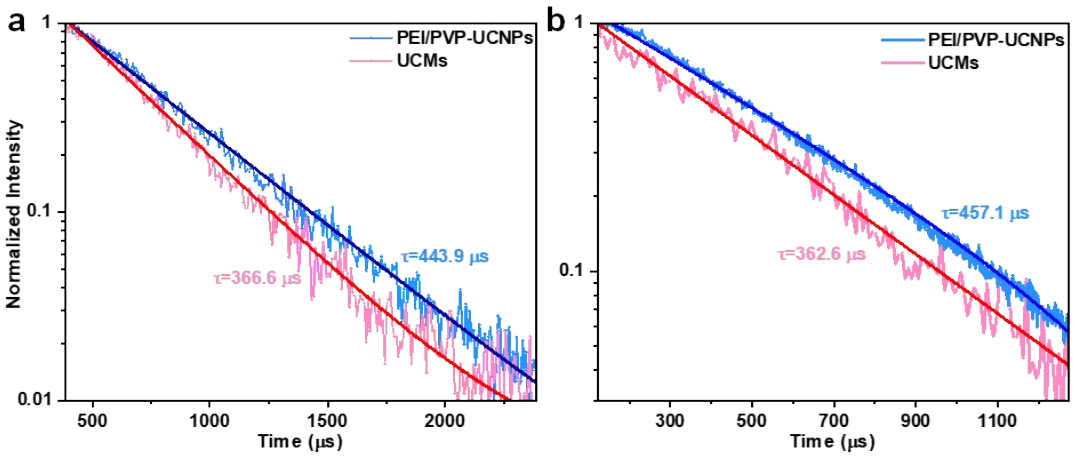

Figure S11. Decay curves and fitted decay times of PEI/PVP-UCNPs and UCMs at (a) 475 nm, and (b) 645 nm.

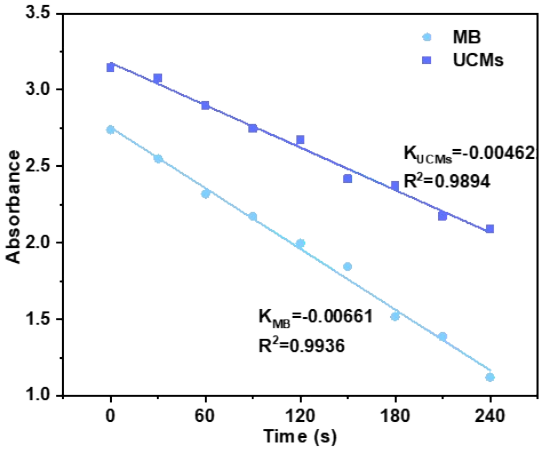

Figure S12. The singlet oxygen ($^1O_2$) quantum yields of UCMs under a 660 nm LED light irradiation (83.2 mW/cm^2).

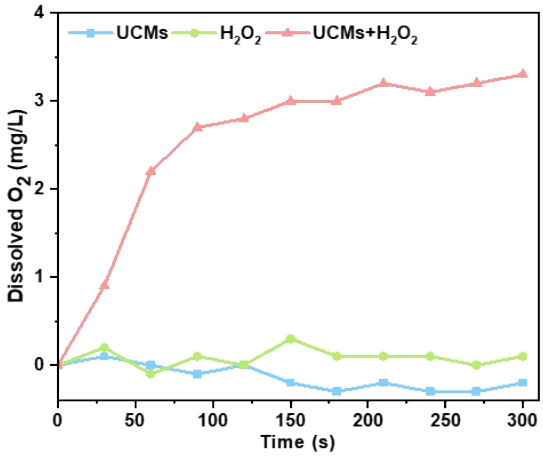

Figure S13. Dissolved oxygen concentrations of UCMs in different conditions measured by a portable dissolved oxygen meter (Rex, JPB-607A, China). The concentration of UCMs was 200 μg/mL, and the concentration of H_2O_2 was 100 μM.

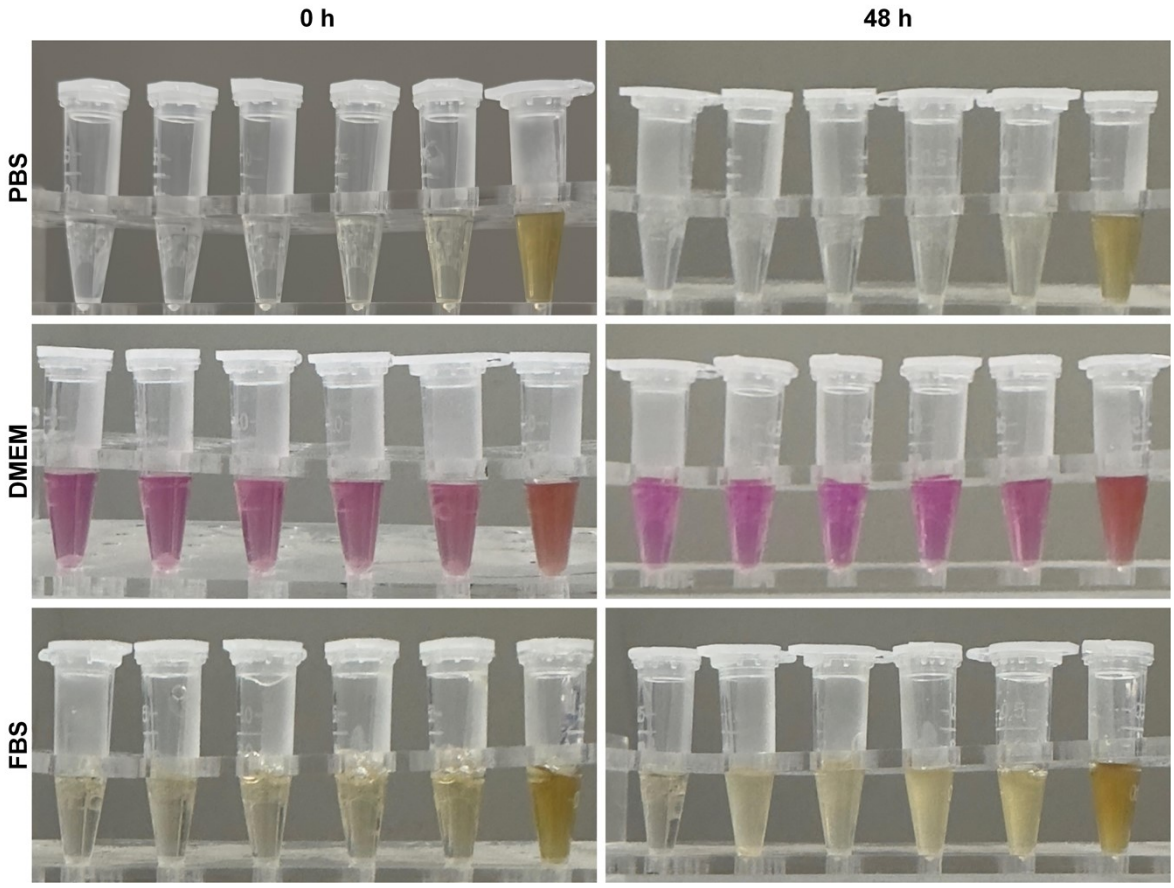

Figure S14. The stability of different concentrations of UCMs in the different solutions such as PBS, DMEM, and FBS. The concentrations of UCMs are 0, 12.5, 25, 50, 100, and 1000 μg/mL, respectively.

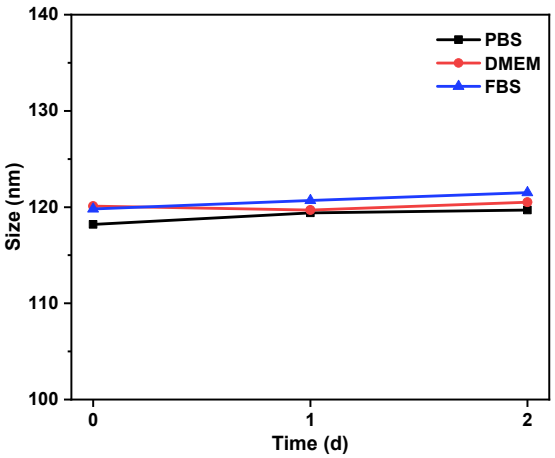

Figure S15. The change of the size of the UCMs in the different environments for two days.

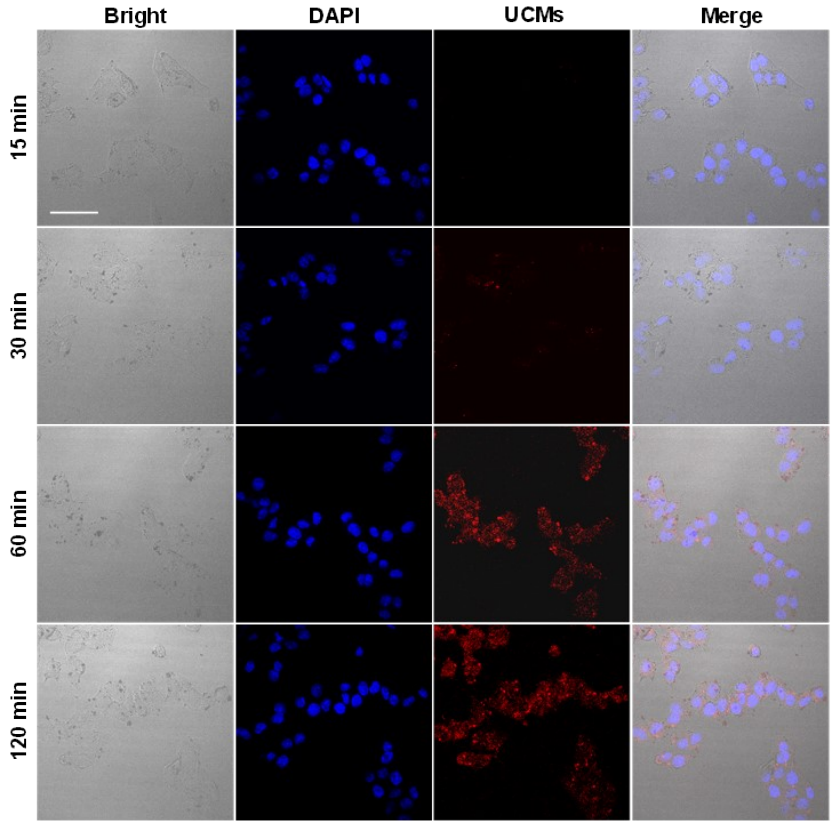

Figure S16. CLSM images of HepG2 cells incubated with UCMs (100 μg/mL) at different time intervals and stained with cell nuclear dye DAPI. The scale bar indicates 50 μm.

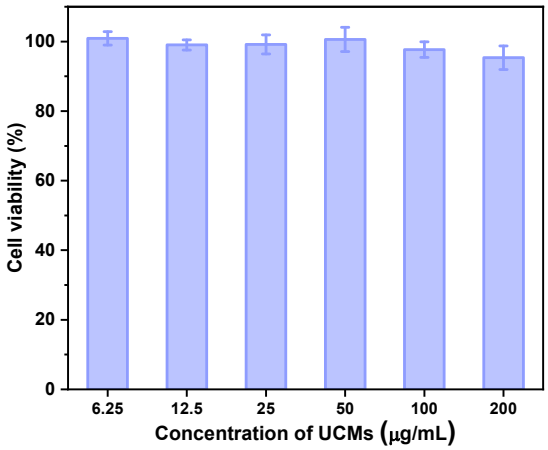

Figure S17. LX-2 cell viability treated with different concentrations of UCMs for 24 h. The data error bars indicate means ± SD (n = 3).

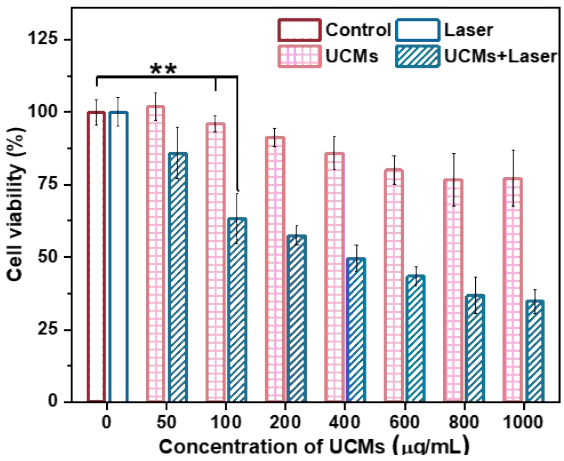

Figure S18. HepG2 cell viability after incubation with different treatments (control, laser, UCMs, UCMs + laser). Data were shown as means ± SD. n = 3. **p < 0.01, ***p < 0.001. (Laser: 980 nm, 1.5 W/cm^2 for 10 min).

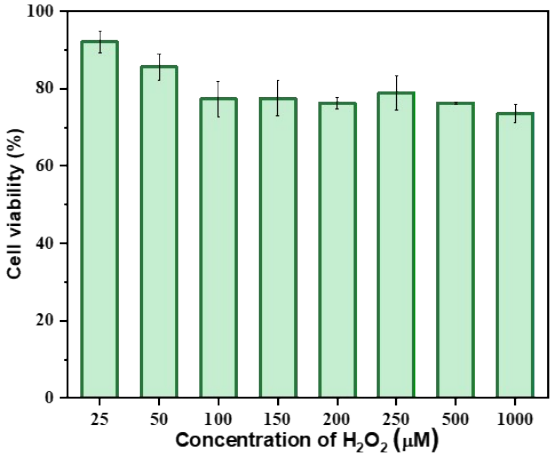

Figure S19. HepG2 cell viability treated with different concentrations of H_2O_2 for 24 h. The data error bars indicate means ± SD (n = 3).

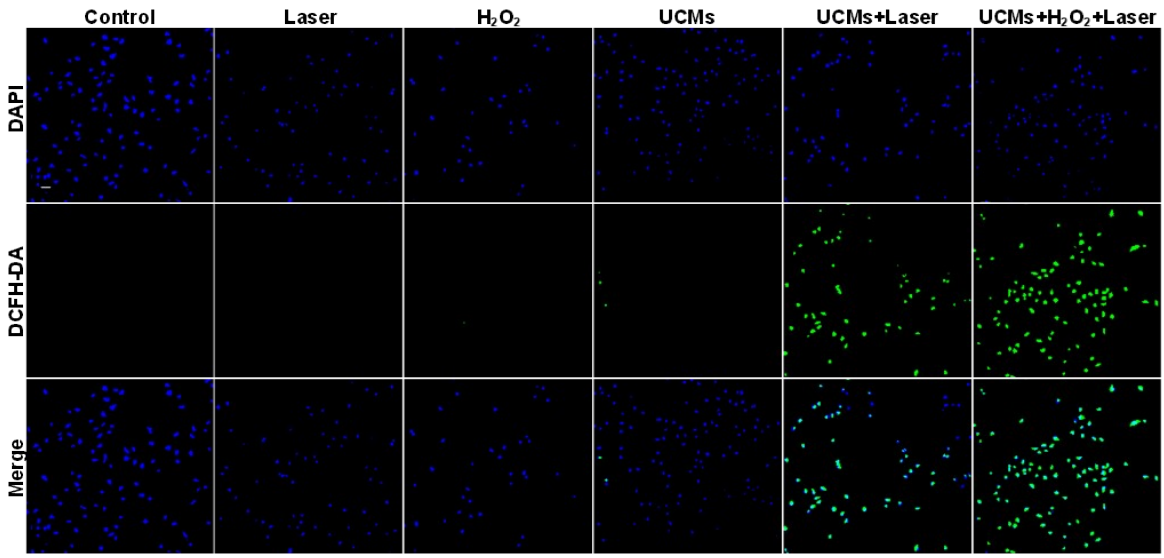

Figure S20. Detection of ROS generation of UCMs in vitro confirmed by DCFH-DA after various treatments. (I) Control, (II) Laser, (III) H_2O_2 (100 μM), (IV) UCMs (100 μg/mL), (V) UCMs (100 μg/mL) + Laser, (VI) UCMs (100 μg/mL) + H_2O_2 (100 μM) + Laser. DAPI for cell nuclear staining. (Laser: 980 nm; 1.5 W/cm^2 for 10 min). The scale bar indicates 50 μm.

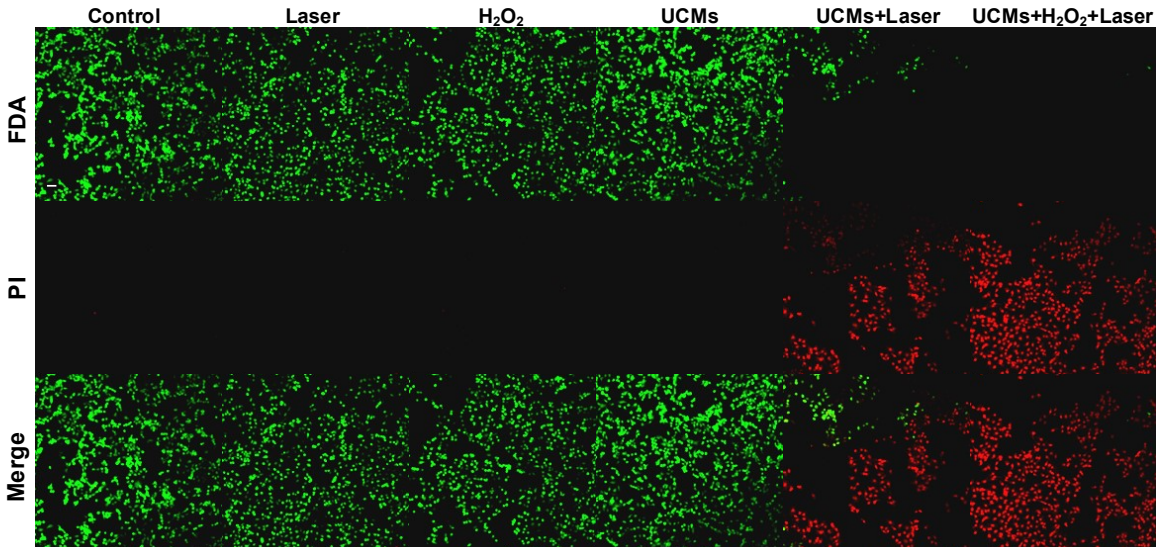

Figure S21. Detection of live/dead cells after various treatments. (I) Control, (II) Laser, (III) H_2O_2 (100 μM), (IV) UCMs (100 μg/mL), (V) UCMs (100 μg/mL) + Laser, (VI) UCMs (100 μg/mL) + H_2O_2 (100 μM) + Laser. Live and dead cells were stained with FDA (green) and PI (red), respectively. (Laser: 980 nm; 1.5 W/cm^2 for 10 min). The scale bar indicates 50 μm.

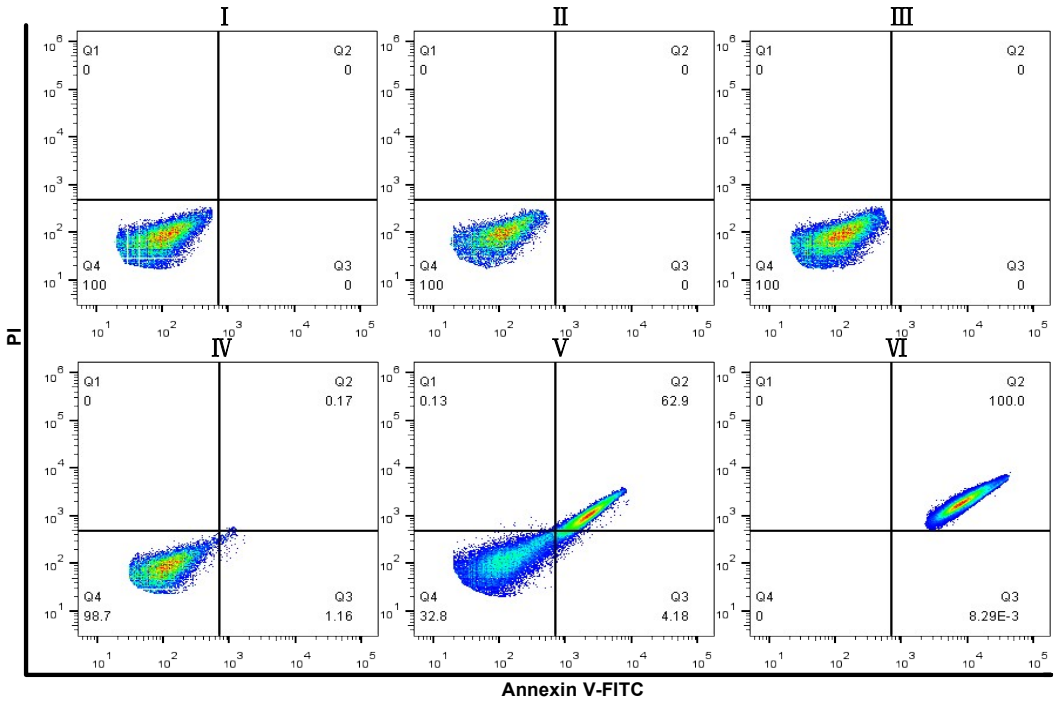

Figure S22. Flow cytometry apoptosis assay of HepG2 cells followed by staining with Annexin-FITC and PI after different treatments: (I) Control, (II) Laser, (III) H_2O_2 (100 μM), (IV) UCMs (100 μg/mL), (V) UCMs (100 μg/mL) + Laser, (VI) UCMs (100 μg/mL) + H_2O_2 (100 μM) + Laser. (Laser: 980 nm, 1.5 W/cm^2 for 10 min).

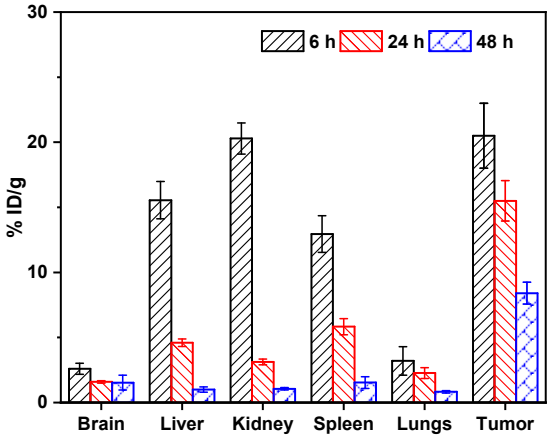

Figure S23. The biodistribution of UCMs in mice after treatment for 6 h, 24 h, and 48 h based on the detection by ICP-MS. %ID/g: percentage injected dose per gram. The data error bars indicate means ± SD (n = 3).

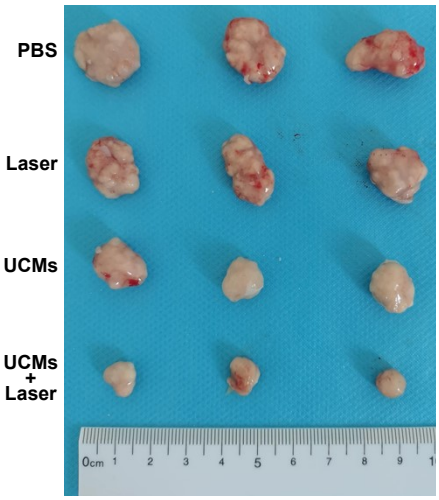

Figure S24. The photographs of tumors extracted from mice after different treatments for 14 days. (UCMs: 4 mg/mL, 100 μL; Laser: 980 nm, 1.5 W/cm^2, 10 min).

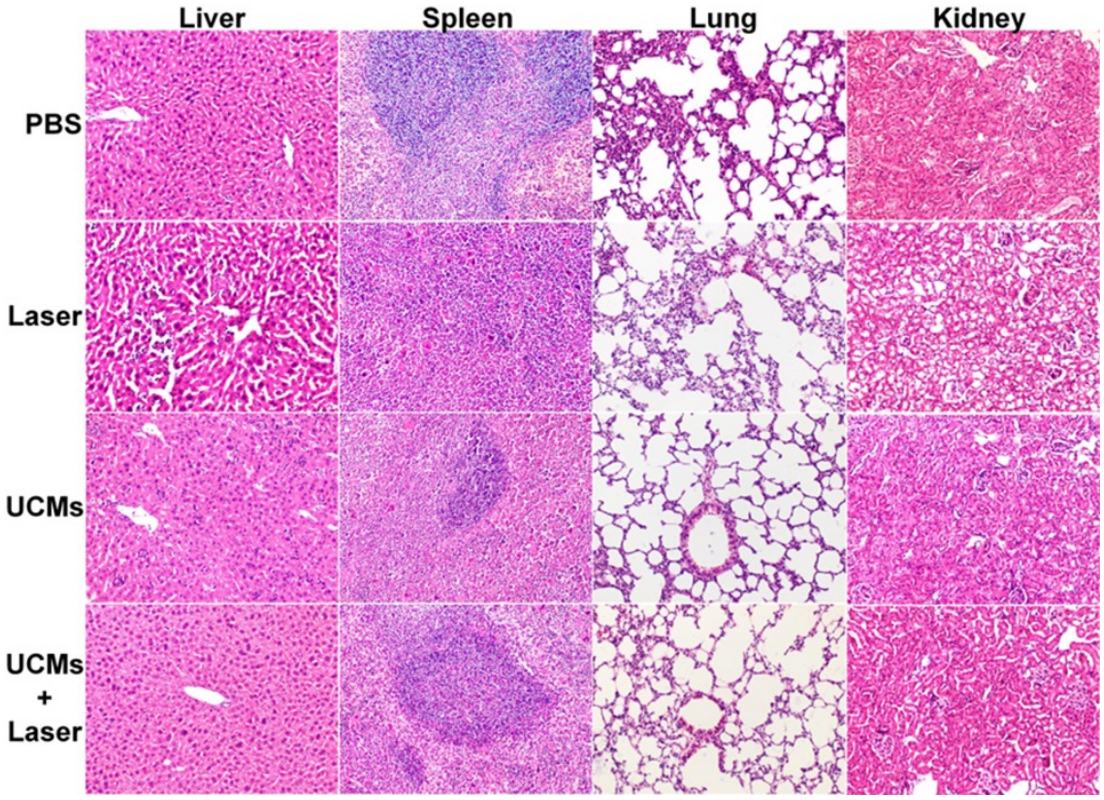

Figure S25. H&E staining on major organs (liver, spleen, lung, and kidney) at the end of the therapy studies. No obvious pathological abnormalities were observed. Scale bar = 50 μm.

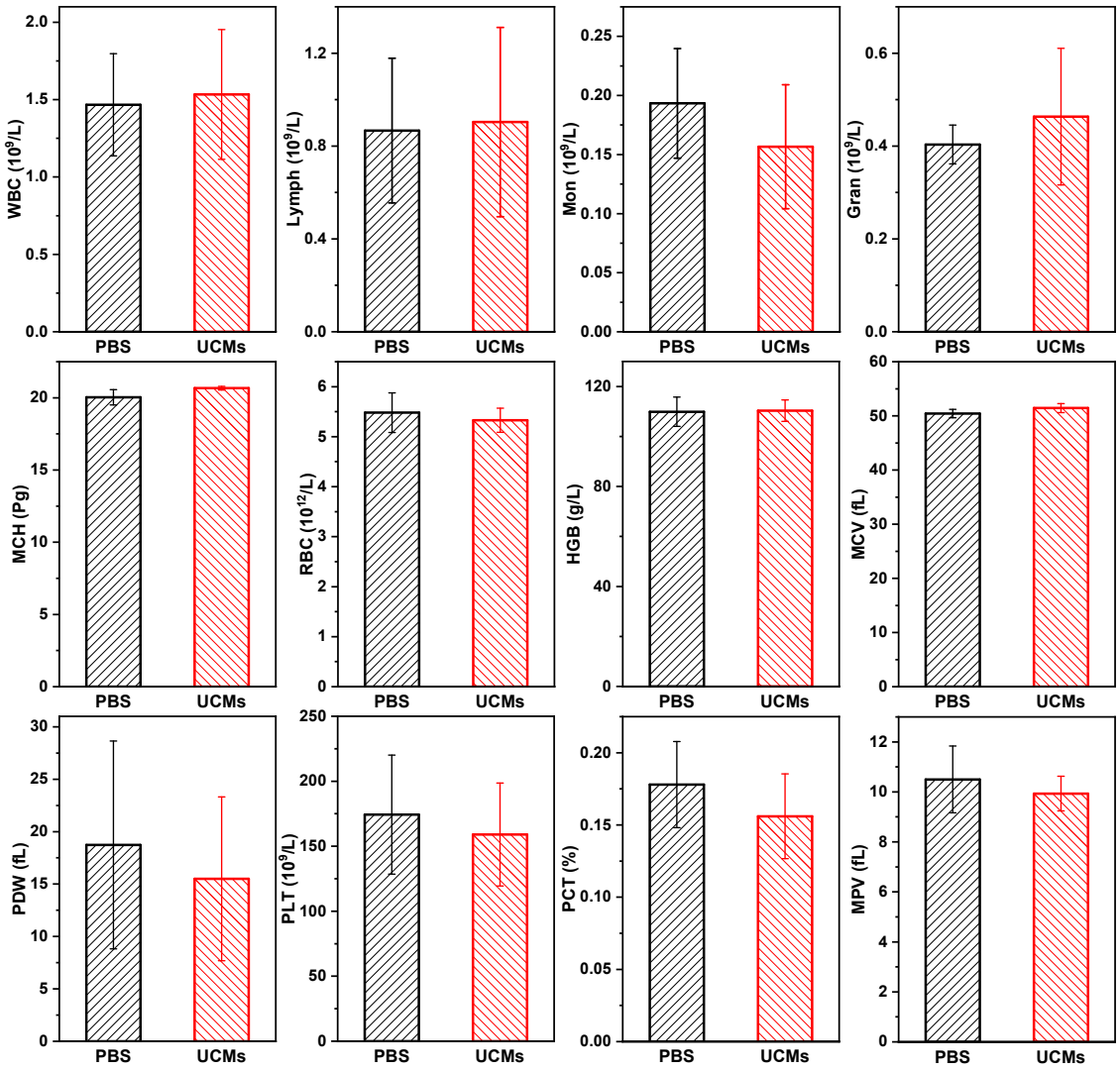

Figure S26. Analysis of whole blood cells of tumor-bearing mice following intravenous UCMs injection. WBC, white blood cell; Lymph, lymphocyte; Mon, monocyte; Gran, granulocyte; MCH, mean corpuscular hemoglobin; RBC, red blood cell; HGB, hemoglobin; MCV, mean corpuscular volume; PDW, platelet distribution width; PLT, platelets; PCT, plateletcrit; MPV, mean platelet volume. Data are represented as mean ± SD; n = 3 samples per group.

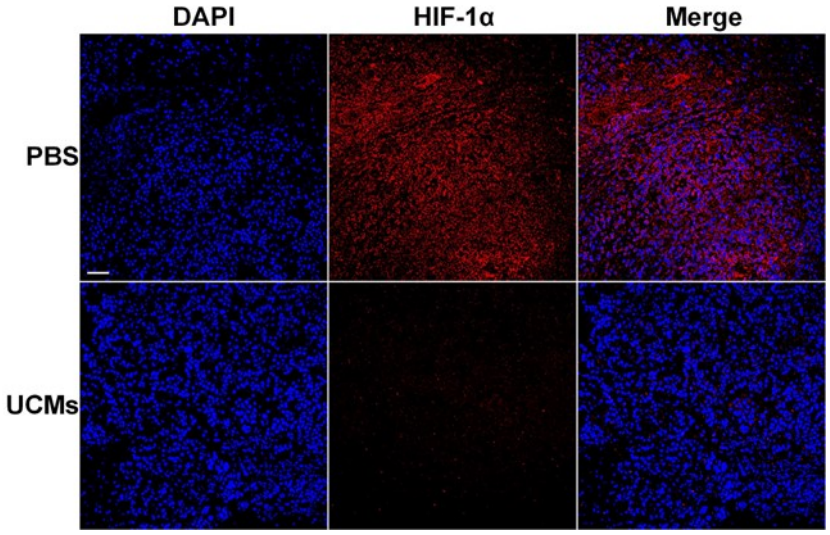

Figure S27. The HIF-1α staining in the tumor site with different treatments (PBS, UCMs: 4 mg/mL, 100μL). DAPI for cell nuclear staining. Scale bar = 50 μm.

Reference

[1] L. Zhang, J. Lei, F. Ma, P. Ling, J. Liu and H. Ju, *Chem. Commun*, 2015, **51**, 10831-10834.

[2] M. K. Ruhi, A. Ak and M. Gülsoy, *Photodiagnosis Photodyn. Ther,* 2018, **21**, 334-343.